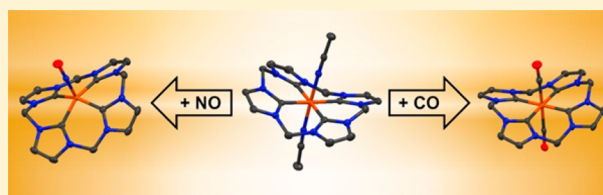


## Synthesis and Characterization of an Iron Complex Bearing a Cyclic Tetra-N-heterocyclic Carbene Ligand: An Artificial Heme Analogue?

Markus R. Anneser,<sup>†</sup> Stefan Haslinger,<sup>†</sup> Alexander Pöthig,<sup>†</sup> Mirza Cokoja,<sup>†</sup> Jean-Marie Basset,<sup>‡</sup> and Fritz E. Kühn<sup>\*†</sup><sup>†</sup>Chair of Inorganic Chemistry/Molecular Catalysis, Catalysis Research Center, Ernst-Otto-Fischer-Strasse 1 and Faculty of Chemistry, Lichtenbergstrasse 4, Technische Universität München (TUM), D-85747 Garching bei München, Germany<sup>‡</sup>KAUST Catalysis Center, King Abdullah University of Science and Technology (KAUST), Thuwal, Kingdom of Saudi Arabia

## Supporting Information

**ABSTRACT:** An iron(II) complex with a cyclic tetradentate ligand containing four N-heterocyclic carbenes was synthesized and characterized by means of NMR and IR spectroscopies, as well as by single-crystal X-ray structure analysis. The iron center exhibits an octahedral coordination geometry with two acetonitrile ligands in axial positions, showing structural analogies with porphyrine-ligated iron complexes. The acetonitrile ligands can readily be substituted by other ligands, for instance, dimethyl sulfoxide, carbon monoxide, and nitric oxide. Cyclic voltammetry was used to examine the electronic properties of the synthesized compounds.



## INTRODUCTION

Iron, one of the most abundant elements on earth, plays a vital role in various biological processes, with prominent examples being the oxygen transport and oxidation of nonactivated hydrocarbons.<sup>1</sup> Mimicking, by artificial systems, these processes found in nature is a goal that has been targeted by chemical research for several decades.<sup>2</sup> In recent years, the use of N-heterocyclic carbene (NHC) ligands on iron centers came into focus, resulting in several reports on the isolation of biologically relevant iron intermediates stabilized by NHC ligands.<sup>3,4</sup> In addition, iron NHC complexes were successfully applied as catalysts for a variety of transformations, with recent examples being the olefin epoxidation and aromatic hydroxylation.<sup>3a,5</sup> Structural variations of iron NHC complexes are manifold, ranging from simple mono(NHC) complexes to compounds bearing chelating ligands with up to four NHC moieties.<sup>3a</sup> Pioneering work on cyclic chelating tetra(NHC) ligands was done by Jenkins and Murphy, who presented synthetic access to 18- and 24-membered macrocyclic tetra(NHC) ligands (Figure 1) and subsequently to a variety of transition metal complexes with the respective ligands.<sup>6,7a,b</sup> In addition to the characterization of a number of new transition metal

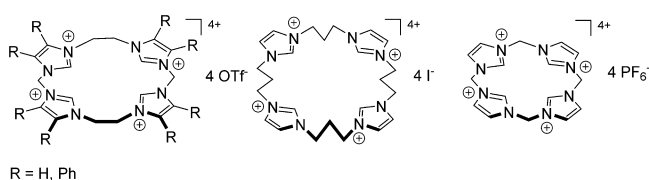


**Figure 1.** Macrocyclic chelating tetra(NHC) ligand precursors reported by Jenkins (left), Murphy (middle), and this work (right).<sup>6,7a</sup>

complexes, Murphy showed that the Ni(II) complex of his ligand is able to catalytically hydrogenate a range of challenging compounds.<sup>7b</sup> Jenkins could show that the Fe(II) complex of his ligand is successfully applicable for the catalytic aziridination of olefins and that an Fe(IV) compound could be identified as active intermediate.<sup>7d,e</sup> Recently Meyer demonstrated that cyclic chelating tetra(NHC) ligands can be used for the stabilization of reactive Fe(IV)oxo species.<sup>8</sup> Metal complexes of the respective smaller 16-membered macrocyclic tetra(NHC) ligand have not been reported until now, although its synthesis was published recently.<sup>9</sup> Because of its structural similarity to naturally occurring ligand systems like porphyrine (by switching its CNC- toward a NCN-motive) it appears to be interesting to evaluate the properties of the respective transition metal complexes. Starting with Fe is reasonable, because the resulting complex could be seen as an artificial analogue of the biological heme unit, with respect to structural and electronic properties (*vide infra*).

Therefore, the synthesis of such a chelating cyclic tetra(NHC) ligand and subsequent isolation of the respective iron(II) complex as an artificial heme analogue was targeted. To investigate possible electronic similarities of such an iron compound with iron porphyrins, axial ligand exchange reactions and their impact on spectroscopic data as well as on electrochemical properties are a valid approach.<sup>10</sup> Especially knowledge about the redox behavior will be of great interest for possible future applications in the field of catalysis. In this work, the preparation of the described tetra(NHC) ligand precursor, the resulting iron(II) complex, and reactions of this complex

Received: December 19, 2014

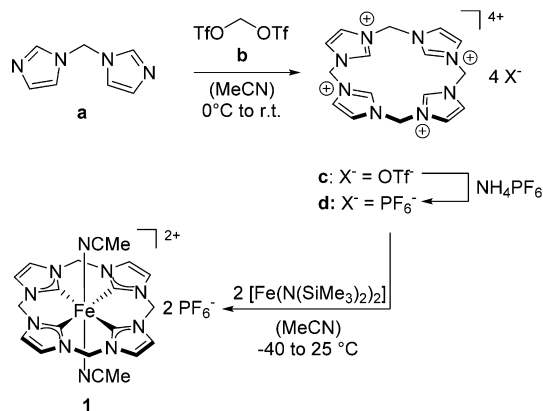
Published: April 6, 2015

with dimethyl sulfoxide (DMSO), carbon monoxide, and nitrogen monoxide are presented. The spectroscopic and electrochemical properties of all reported iron complexes are compared to literature-known iron compounds, revealing a rather unusual behavior of the described iron(II) tetra(NHC) complex.<sup>3a,11–16</sup>

## RESULTS AND DISCUSSION

**Synthesis of Iron(II) Tetra(NHC) Complex 1.** The preparation of calix[4]imidazolium triflate (**c**) and hexafluorophosphate (**d**) salts follows a modified, halogen-free pathway of a recently published synthesis protocol.<sup>9</sup> Starting from methylene bisimidazole **a** and methylene bis-(trifluoromethane)sulfonate **b**, the tetracarbene precursor **d** was obtained in yields of up to 70% (Scheme 1). Sulfonate **b** was obtained from the reaction of triflic acid anhydride and paraformaldehyde, allowing for the isolation of tetra-(imidazolium) salts in good yields.

**Scheme 1.** Synthesis of the Calix[4]imidazolium Salts **c** and **d** and Subsequent Reaction of **d** with  $[\text{Fe}\{\text{N}(\text{SiMe}_3)_2\}_2]$  to Form Fe(II) Complex **1**



The iron bisamide  $[\text{Fe}\{\text{N}(\text{SiMe}_3)_2\}_2]$  is a viable precursor for the synthesis of iron(II) NHC complexes.<sup>8,17</sup> An excess of the iron precursor is used to ensure a quantitative deprotonation of the tetra(imidazolium) salt **d** (Scheme 1), resulting in the formation of  $[\text{Fe}(\text{MeCN})_6](\text{PF}_6)_2$  (see Supporting Information for details) as iron-containing byproduct. Removal of the latter was achieved via column chromatography over dried silica under inert gas atmosphere, and **1** could be isolated on a multigram scale in yields >90% as yellow powder. Complex **1** is a low-spin complex and is therefore diamagnetic; hence, NMR spectroscopy is possible. In the  $^1\text{H}$  NMR spectra of **1** the presence of two singlet peaks indicates fast inversion of the cyclic tetra(NHC) ligand (compare **3**). Various temperature  $^1\text{H}$  NMR experiments do not show significant line broadening even at  $-40^\circ\text{C}$  in acetonitrile. In acetone, where exchange of bound acetonitrile is slow on a NMR-time scale (bound  $\text{CH}_3\text{CN}$  at 1.70 ppm; see Supporting Information), only a slight line broadening of the  $\text{CH}_2$  signal is observed. This proves fast inversion of the ligand in case of complex **1**. The signal of the backbone protons of the NHC moieties appears at 7.57 ppm and the signal of the methylene bridges at 6.29 ppm. For the coordinating carbon atoms a signal at 205 ppm is identified by  $^{13}\text{C}$  NMR, which is in the expected range for iron carbene complexes (180 to 210 ppm).<sup>17a,18</sup>

Additionally, **1** was characterized by single-crystal X-ray diffraction (XRD). Slow diffusion of diethyl ether into an acetonitrile solution of **1** gave suitable single crystals. The solid-state structure shows a distorted octahedral coordination mode of the iron center with the tetradentate cyclic ligand coordinated in square-planar fashion (Figure 2).

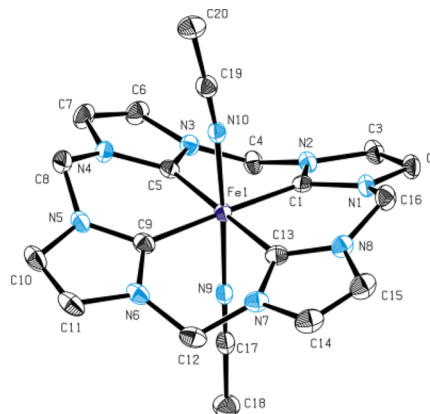
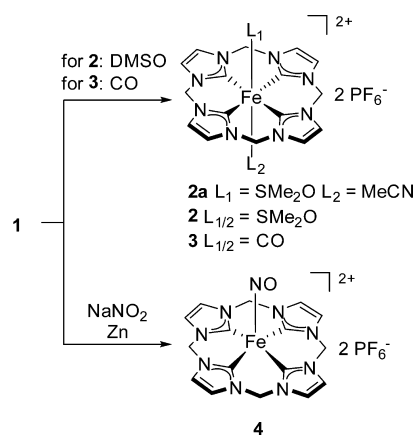


**Figure 2.** ORTEP-style drawing of the cationic fragment of compound **1**. Hydrogen atoms and two  $\text{PF}_6^-$  anions are omitted for clarity, and thermal ellipsoids are shown at a 50% probability level. Selected bond lengths ( $\text{\AA}$ ) and angles (deg): Fe1–C1 1.912(3), Fe1–C5 1.904(3), Fe1–N9 1.930(1), Fe1–N10 1.933(1), N9–C17 1.140(1), N10–C19 1.133(1), C1–Fe1–C5 90.31(2), N9–Fe1–N10 177.08(3), Fe1–N9–C17 173.25(3), Fe1–N10–C19 177.50(4).

The Fe– $\text{C}_{\text{NHC}}$  distances of **1** with its saddle-distorted ligand conformation average to 1.907  $\text{\AA}$ , which is slightly shorter than for comparable Fe(II) tetracarbenes ( $\sim 2.01 \text{\AA}$ ).<sup>7c,8</sup> As this can be attributed to the methylene bridges instead of the longer ethylene bridges in case of the literature-known complexes, the Fe– $\text{C}_{\text{NHC}}$  distances in these complexes apparently depend at least in part on the shape of the tetradentate ligand. Thermogravimetric analysis revealed decomposition of solid **1** under inert atmosphere at  $120^\circ\text{C}$ , initiated by dissociation of the axial acetonitrile ligands.

**Reactivity of Iron(II) Tetra(NHC) Complex 1.** The reactivity of **1** was investigated by introducing DMSO, CO, and NO as axial ligands (Scheme 2). Addition of excess DMSO to an acetonitrile solution of **1** yields a mixture of the mono-

**Scheme 2.** Synthesis of Complexes **2–4**, Employing Ligand-Exchange Reactions on **1**



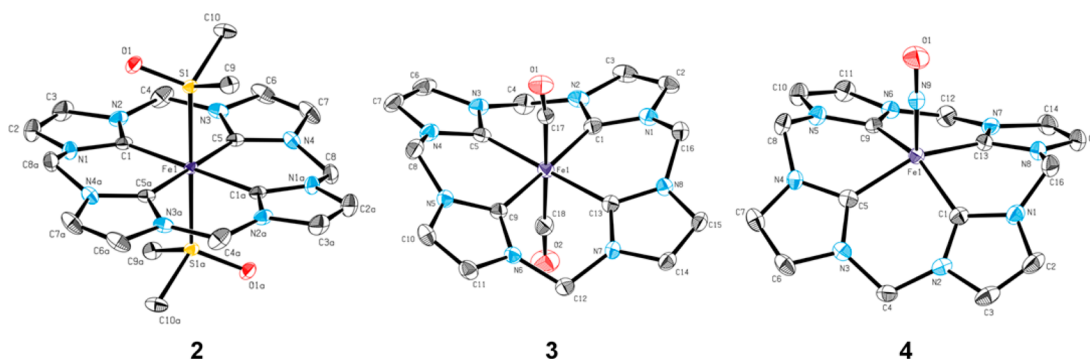


**Figure 3.** ORTEP-style drawing of the cationic fragment of compounds 2–4. Hydrogen atoms and  $\text{PF}_6^-$  anions are omitted for clarity, and thermal ellipsoids are shown at a 50% probability level. Selected bond lengths (Å) and angles (deg): 2: Fe1–C1 1.936(3), Fe1–C5 1.938(3), Fe1–S1 2.205(1), S1–O1 1.479(1), C1–Fe1–C5 90.41(2). Symmetry code (a):  $-x + 2, -y + 1, -z + 2$ ; 3: Fe1–C1 1.915(3), Fe1–C5 1.913(3), Fe1–C17 1.826(1), C17–O1 1.127(1), Fe1–C18 1.815(1), C18–O2 1.128(1), C1–Fe1–C5 89.27(10), C1–Fe1–C13 90.21(10), Fe1–C18–O2 177.39(3), Fe1–C17–O1 173.14(3); C18–Fe1–C17 177.11(2); 4: Fe1–C1 1.950(3), Fe1–C5 1.952(3), Fe1–N9 1.673(2), N9–O1 1.159(3), C1–Fe1–C5 86.77(10), Fe1–N9–O1 172.13(10).

and bis(DMSO) derivatives **2a** and **2** (see Supporting Information for  $^1\text{H}$  NMR assignment). If acetone is used as noncoordinating solvent, solely the bis(DMSO) complex **2** is obtained. Bis(carbonyl) complex **3** can be accessed in 77% yield by stirring **1** under a CO pressure of 2.5 atm at 40 °C. This is a rare example of a stable, cationic iron NHC complex with CO ligands.<sup>3a,11,12</sup> Typically, only monocarbonyl derivatives of iron(II) complexes bearing neutral tetradentate ligands with NHC moieties are known.<sup>17a</sup> Examples for iron dicarbonyl complexes have been reported for heme systems.<sup>12c,19</sup> The isolation of an iron complex with two trans-standing CO ligands indicates high electron density at the iron center, resulting from the strong  $\sigma$ -donor ability of the four NHC moieties.

Nitric oxide, generated *in situ* from  $\text{NaNO}_2$  and Zn, can be used to convert **1** to the square-pyramidal nitrosyl complex **4** in 73% yield as green solid. Addition of Zn is necessary to avoid unproductive reduction of  $\text{NaNO}_2$  by **1**. Apart from Zn, also iron powder and hydroquinone were successfully applied as reducing agents. In analogy to **1**, complexes **2–4** were characterized in solid-state by single-crystal XRD (Figure 3).

Both **2** and **3** exhibit a distorted octahedral geometry of the iron center with both acetonitrile ligands being replaced by DMSO or CO, respectively. Regarding the ligand conformation, in case of **2** the tetra(NHC) ligand is almost planar, whereas it is saddle-distorted for **3** in analogy to starting complex **1**. Interestingly, nitrosyl derivative **4** shows a pentacoordinated iron center in a tetragonal-pyramidal geometry with the iron atom being located 0.475 Å above the plane, which is spanned by the tetradentate ligand. Consequently, the tetra(NHC) ligand is forced into a ruffled conformation. This is the first example of such a coordination behavior for nitrosyl Fe NHC complexes, and it expands the field of Fe nitrosyl compounds, which typically bear anionic ligands with nitrogen donor atoms or porphyrinato ligands.<sup>13,15,16</sup>

Compared to **1**, the Fe– $\text{C}_{\text{NHC}}$  bond lengths do not change significantly upon axial ligand replacement to form **2** and **3** (Fe– $\text{C}_{\text{NHC}}$  = 1.90 to 1.94 Å). Although the coordination geometry changes significantly, nitrosyl derivative **4** exhibits only negligibly larger Fe– $\text{C}_{\text{NHC}}$  bond lengths of 1.95 Å. The molecular structure of **2** reveals coordination of the DMSO ligands in axial positions via the sulfur atoms, which is also found for heme Fe(II) compounds and other electron-rich

nonheme iron complexes.<sup>20</sup> The Fe–S distance in **2** is determined with 2.205(1) Å and the S–O bond length with 1.479(1) Å, which is characteristic for S-bound DMSO.<sup>20,21</sup> In the case of dicarbonyl-substituted complex **3**, the molecular structure reveals two non equal carbonyls in the solid state, reflected by the Fe–C bond lengths of 1.815(1) Å and 1.826(1) Å as well as by the Fe–C–O bond angles of 177.39(3)° and 173.11(3)°, respectively. These values are in good accordance with those reported for other Fe NHC carbonyl complexes.<sup>17a,18</sup> Single-crystal XRD of Fe nitrosyl complex **4** revealed a molecular structure that exhibits an Fe–N bond length of 1.673(2) Å, an N–O bond length of 1.159(3) Å (free NO:<sup>22</sup> 1.14 Å), and an Fe–N–O angle of 172.13(10)°. Notably, the N–O bond length is in the range of known heme (1.16 to 1.18 Å) and nonheme (1.11 to 1.15 Å) {FeNO}<sup>7</sup> compounds,<sup>14,16a</sup> but the Fe–N distance is significantly shorter than usually observed, for both heme (1.74 to 1.78 Å) and comparable nonheme compounds (1.71 to 1.75 Å).<sup>14</sup> However, several anionic FeNO compounds with comparable or even shorter Fe–N distances (1.60 to 1.70 Å) are known.<sup>23</sup> Additionally, a bond angle close to 180° is usual for an Fe–N bond order >1, and together with the prolonged N–O bond length, our findings indicate strong back bonding, lowering the formal N–O bond order to ~2 (theoretical value: 1.16 Å).<sup>3b,22,24</sup>

In solution,  $^1\text{H}$  NMR spectra of **2** and **3** are comparable to the data of **1** with two singlet peaks for the tetra(NHC) ligand. The chemical shifts are slightly different, being (**2**) 6.50 and (**3**) 6.27 ppm for the methylene bridges (**1**: 6.29 ppm) and (**2**) 7.64 and (**3**) 7.55 ppm for the backbone protons of the NHC moieties, respectively (**1**: 7.57 ppm). The difference in chemical shifts is larger for the coordinating carbon atoms as determined by  $^{13}\text{C}$  NMR, being 189 ppm for **2** and 179 ppm for **3** (**1**: 205 ppm). On NMR scale, an equilibrium for the coordination and dissociation of the DMSO ligands in axial positions of **2** is observed in acetonitrile solution. Depending on the amount of DMSO added to a solution of **1** in acetonitrile, a mixture of **1**, **2**, and a mono(DMSO)-substituted derivative **2a** is obtained. With only a slight excess of DMSO (less than 6 equiv) being used, all three species exist at the same time, while the equilibrium is shifted toward **2** and **2a** with larger amounts of DMSO. Compound **2** is observed almost exclusively with more than 50 equiv of DMSO (see Supporting Information for details). The presence of two different axial ligands in case of **2a**



causes the protons of the methylene groups to split into doublets in the  $^1\text{H}$  NMR spectrum. Also, the  $\text{CH}_3$  groups of the coordinated DMSO are identified with a chemical shift of 4.50 ppm in the  $^1\text{H}$  NMR spectrum (free DMSO:<sup>25</sup> 2.50 ppm). This observation is in accord with literature values for S-bound DMSO.<sup>20,21</sup>

Despite the fact that **4** is a 17 valence-electron complex, it was possible to collect sharp and not paramagnetic-shifted NMR data. Such sharp signals are uncommon for  $\{\text{FeNO}\}^7$  complexes (Enemark–Feltham notation); detailed investigations concerning the reasons of the observed behavior are ongoing in our group.<sup>15,26</sup> In the  $^1\text{H}$  NMR spectrum, the methylene bridge causes two overlapping doublet signals for each proton with chemical shifts of 6.46 and 6.52 ppm, whereas the NHC backbone protons are represented by a singlet at 7.78 ppm. The  $^{13}\text{C}$  NMR spectrum shows the coordinated carbon atom with an unusual upfield shift for iron carbene complexes of 170 ppm. Interestingly, **4** also exhibits a distinct X-band EPR signal with  $g = 1.99$  (see Supporting Information), which is in accordance with previously reported  $\{\text{FeNO}\}^7$  complexes.<sup>15,27</sup>

In addition to XRD and NMR, IR spectra were recorded for all complexes as X–O bond vibrations—with X being the coordinating atom, for example, C in case of CO or S in case of DMSO—are a characteristic attribute for the electronic situation at the metal center. Complex **1** exhibits a weak band at  $2291\text{ cm}^{-1}$  for the C–N stretching vibration of the coordinated acetonitrile molecules, reflecting  $\pi$ -back-bonding from the iron center as the value of  $2291\text{ cm}^{-1}$  is at the lower end of the typical range for metal-bound acetonitrile vibrations ( $2330$  to  $2290\text{ cm}^{-1}$ ).<sup>21</sup> IR spectroscopy of **2** revealed an intense band at  $1100\text{ cm}^{-1}$  (Table 1), which is absent for compound **1** and which can be assigned to the S–O stretching band of the coordinated DMSO.<sup>21,28</sup>

**Table 1.** X–Y Stretching Frequencies of Axial Ligands, X–Y Bond Lengths, and Fe–X–Y Angles for **1** and **2–4** (X = N (**1** and **4**), S (**2**), and C (**3**); Y = C (**1**) and O (**2–4**))

	$\nu(\text{X–Y})$ [ $\text{cm}^{-1}$ ]	X–Y [ $\text{\AA}$ ]	Fe–X–Y [deg]
<b>1</b>	2291	1.14	178/173
<b>2</b>	1100	1.48	115
<b>3</b>	2010	1.13	173/177
<b>4</b>	1729	1.16	172

Bis(carbonyl) complex **3** exhibits sharp CO band at  $2010\text{ cm}^{-1}$  (free CO:<sup>24</sup>  $2143\text{ cm}^{-1}$ ). This value is slightly lower than typically found for Fe(II) NHC carbonyl complexes ( $2050$  to  $1985\text{ cm}^{-1}$ ) and is close to the vibration frequencies observed for  $\text{Fe}(\text{CO})_5$  ( $2024$  and  $2014\text{ cm}^{-1}$ ) or heme dicarbonyls ( $2021$  and  $2016\text{ cm}^{-1}$ ).<sup>19,29</sup> Therefore, strong  $\pi$ -back-bonding apparently occurs in case of **3**. This is understood as a direct consequence of the strong  $\sigma$ -donating properties of the tetra(NHC) ligand, inducing high electron density at the iron center. In case of nitrosyl complex **4**, an NO stretching vibration is observed at  $1729\text{ cm}^{-1}$ . The latter value is slightly higher than typically found for heme  $\{\text{FeNO}\}^7$  complexes ( $\sim 1600$  to  $1700\text{ cm}^{-1}$ ) but in the range of nonheme  $\{\text{FeNO}\}^7$  complexes ( $1639$  to  $1840\text{ cm}^{-1}$ ).<sup>14,16</sup>

**Electrochemical Investigations.** In order to gain further insight into the electronic structure of the described Fe NHC compounds, cyclic voltammetry (CV) measurements were performed in acetonitrile solution with tetrabutylammonium hexafluorophosphate as the supporting electrolyte. Complexes **1** and **3** show a one-electron redox process, which is assigned to the Fe(II)/Fe(III) redox couple. It is fully reversible for at least 20 cycles in case of **1** and quasi-reversible in case of **3**. In acetonitrile solution, **2** dissociates into a mixture of **1**, **2a**, and **2** (see Supporting Information). As a consequence a voltammogram showing the oxidation peaks for all of the three species is obtained in acetonitrile. Nitrosyl complex **4** is not oxidized but undergoes an irreversible reduction (Figures 4 and 5).

For the fully reversible oxidation of complex **1** and the quasi-reversible oxidation of **3** the half-cell potentials  $E_{1/2}$  were determined with 0.15 and 1.25 V, respectively. The peak separation  $\Delta E_p$  with 91 mV for **1** and 140 mV for **3** is only slightly above the typical value (80 mV) for a reversible one-electron process.<sup>30</sup> Compared to previously studied Fe(II) NHC complexes bearing tetradentate ligands with only two NHC moieties and axial acetonitrile ligands ( $E_{1/2} = 0.40$  to  $0.52\text{ V}$ ), the value of 0.15 V obtained for **1** is remarkably low.<sup>17a</sup> With respect to the strong  $\sigma$ -donating properties of NHC ligands, the low half-cell potential is a direct consequence of the high electron density at the iron center of **1**, which is induced by the tetra(NHC) ligand. However, if approximately 10 equiv of DMSO are added, three quasi reversible oxidation peaks at an oxidation potential of 0.20 V (**1**), 0.45 V (**2a**), and 0.74 V (**2**) can be observed. This observation is in agreement with the

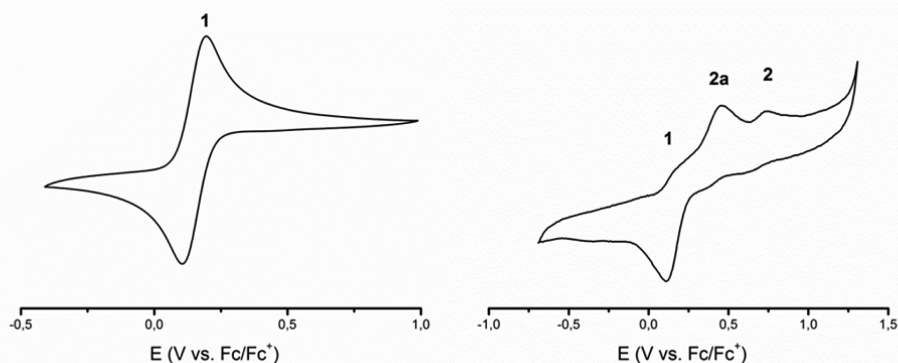


**Figure 4.** Cyclic voltammograms of complexes **1** (left) and **2** (right). Half-cell potentials are determined to  $E_{1/2} = 0.15\text{ V}$  (**1**), and oxidation/reduction potentials are determined to be  $E_{\text{ox}} = 0.20$  (**1**),  $0.45$  (**2a**), and  $0.74\text{ V}$  (**2**);  $E_{\text{red}} = 0.11\text{ V}$  (**1**). Compound **2a** is a mono-DMSO derivative of **2**, bearing one DMSO and one acetonitrile ligand in the axial positions. All potentials are given relative to the half-cell potential of the  $\text{Fc}/\text{Fc}^+$  redox couple.

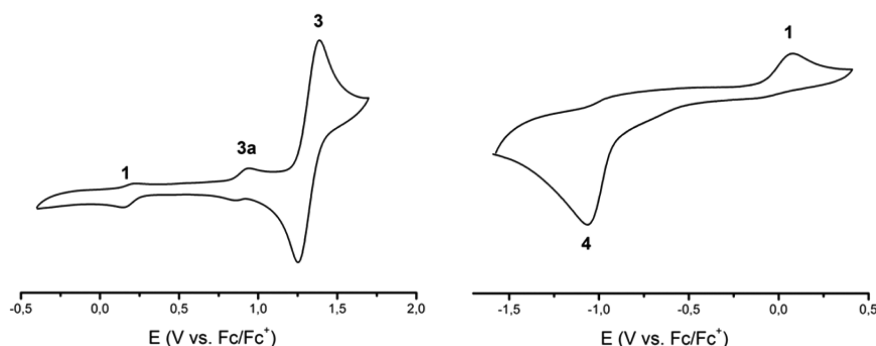


**Figure 5.** Cyclic voltammograms of complexes **3** (left) and **4** (right). Half-cell potentials are determined as  $E_{1/2} = 0.15$  (**1**),  $0.83$  (**3a**), and  $1.25$  V (**3**). Compound **3a** is a monocarbonyl derivative of **3**, bearing one carbonyl and one acetonitrile ligand in the axial positions. The irreversible reduction of **4** occurs at  $-1.06$  V. All potentials are given relative to the half-cell potential of the  $\text{Fc}/\text{Fc}^+$  redox couple.

acetonitrile/DMSO exchange experiments reported above. Interestingly only one reduction potential occurs at  $= 0.11$  V (**1**). This indicates that in case of oxidized **1** ( $\text{Fe(III)}$ ) almost exclusively acetonitrile is coordinating to the metal center under these conditions. This is most likely the result of a switch in the DMSO coordination mode from S- to O-bonding, which has been reported for  $\text{Fe(II/III)}$  heme systems before.<sup>20a</sup>

An exchange of the axial acetonitrile ligands with the strong  $\pi$ -acceptor CO (**3**) results in a drastic shift of  $E_{1/2}$  from  $0.15$  to  $1.25$  V ( $\Delta E_{1,3} = 1.10$  V), as the electron density at the iron center is lowered significantly due to  $\pi$ -back-bonding to the carbonyl ligands (Figure 5). During cyclic voltammetry experiments with **3**, minor decomposition is indicated by appearance of the respective peaks for the reversible oxidation of **1** at  $E_{1/2} = 0.15$  V after several cycles (see Supporting Information). Under the conditions for the collection of cyclic voltammetry data the CO ligands dissociate over time and are replaced by acetonitrile to form **1**. At scan rates of at least  $400$  mV/s during CV experiments with **3**, an additional compound is observed at  $E_{1/2} = 0.83$  V ( $\Delta E_p = 85$  mV), which occurs as intermediate during the decomposition of **3** to **1** and can be assigned to a monocarbonyl complex **3a** (see Supporting Information for details).

Contrary to known  $\{\text{FeNO}\}^7$  complexes, no oxidation of **4** is observed in the accessible potential range, which is a consequence of the strong bond between the Fe center and NO.<sup>14b,15</sup> However, an irreversible NO-centered reduction occurred at  $-1.06$  V. Typically, heme  $\{\text{FeNO}\}^7$  complexes are reduced to the respective  $\{\text{FeNO}\}^8$  compounds in the range from  $-0.1$  to  $-0.9$  V.<sup>14b,15</sup> The reduction potential of  $-1.06$  V is slightly out of this range, and just another indicator for the strong  $\sigma$ -donor properties of the tetra(NHC) ligand, leading to an unusually electron-rich  $\text{Fe(II)}$  center. Under CV conditions, the irreversibility of the reduction of **4** indicates that the strength of the Fe–NO bond is lowered significantly, and therefore the  $\{\text{FeNO}\}^8$  species is no longer stable. This is supported by the formation of **1** with its characteristic half-cell potential ( $E_{1/2} = 0.15$  V) after the first cycle during CV experiments, resulting from an  $\text{NO}^-$ -release of the  $\{\text{FeNO}\}^8$  form (see Supporting Information).

Overall, the CV experiments show the good  $\sigma$ -donor abilities of the tetra(NHC) ligand and the high redox stability of the  $\text{Fe(NHC)}_4$  unit. Additionally, the impact of the axial ligands is seen, shifting the oxidation potential from  $0.20$  V (**1**) over  $0.45$  V (**2a**) and  $0.74$  V (**2**) to  $1.30$  V (**3**) and lowering the reduction potential from  $0.11$  V (**1**) to  $-1.06$  V (**4**). It is also shown that the exchange of strongly bound ligands as CO and NO (but

also DMSO) is facilitated by electrochemical oxidation or reduction, respectively.

## CONCLUSION

Four  $\text{Fe(II)}$  complexes bearing a cyclic tetra(NHC) ligand were isolated and investigated, showing electron-rich metal centers as a consequence of the strong  $\sigma$ -donor ability of NHC ligands. The nature of the derivatives with DMSO, CO, or NO ligands in the axial positions proves the high electron density, for example, in case of the carbonyl-substituted complex **3**. The C–O stretching vibrations indicate unusually strong  $\pi$ -back-bonding, as it is known for heme carbonyls. DMSO is coordinated via a sulfur atom instead of an oxygen atom, and stable NO complexes are formed, as expected for electron-rich metal centers. With respect to the electrochemical properties determined by cyclic voltammetry, the Fe tetra(NHC) complexes are all slightly out of the range of comparable complexes that are known in the literature. For example, the half-cell potential of **1** ( $0.15$  V) is significantly lower than those of comparable complexes and the nitrosyl derivative **4** is reduced at  $-1.06$  V (typical range:  $-0.1$  to  $-0.9$  V). Regarding iron-based systems in nature, which are used as oxidation catalysts, electron-rich iron complexes are of high interest, as they might be applicable as artificial, bioinspired catalytic systems for a variety of transformations. A deeper understanding of the manipulation of the electronic structure of such complexes will help to improve the quality of artificial, bioinspired iron systems for various applications. Currently, this class of compounds is investigated in detail for possible applications, particularly in oxidation catalysis, in our laboratories.

## EXPERIMENTAL SECTION

**General Remarks.** Unless otherwise stated, all manipulations were performed under an argon atmosphere using standard Schlenk and glovebox techniques. Solvents were obtained water- and oxygen-free from an Mbraun solvent purification system. Acetonitrile- $d_3$  was refluxed over phosphorus pentoxide and distilled prior to use. The iron bisamide precursor  $[\text{Fe}\{\text{N}(\text{SiMe}_3)_2\}_2(\text{THF})]$  (THF = tetrahydrofuran) and methylene-bisimidazole **a** were synthesized according to known literature procedures.<sup>31,32</sup> All other reagents were purchased from commercial suppliers and were used without further purification. NMR spectra were recorded on a Bruker Avance DPX 400 ( $^1\text{H}$  NMR,  $400.13$  MHz;  $^{13}\text{C}$  NMR,  $100.53$  MHz;  $^{19}\text{F}$  NMR,  $376.49$  MHz), and chemical shifts are reported relative to the residual signal of the deuterated solvent. IR spectra were recorded on a Varian GladiATR IR spectrometer from solid samples. Elemental analyses (C/H/N) were obtained by the microanalytical laboratory at the Technische

Table 2. Crystallographic Data for Fe NHC Complexes 1–4

	1	2	3	4
formula	C <sub>24</sub> H <sub>28</sub> F <sub>12</sub> FeN <sub>12</sub> P <sub>2</sub>	C <sub>24</sub> H <sub>40</sub> F <sub>12</sub> FeN <sub>8</sub> O <sub>2</sub> PS <sub>2</sub>	C <sub>18</sub> H <sub>16</sub> F <sub>12</sub> FeN <sub>8</sub> O <sub>2</sub> P <sub>2</sub>	C <sub>18</sub> H <sub>19</sub> F <sub>12</sub> FeN <sub>10</sub> OP <sub>2</sub>
fw	830.37	978.66	722.18	737.18
color/habit	yellow/fragment	yellow/fragment	yellow/plate	green/fragment
crystal dimens [mm <sup>3</sup> ]	0.10 × 0.15 × 0.33	0.15 × 0.30 × 0.42	0.14 × 0.28 × 0.38	0.16 × 0.17 × 0.46
crystal system	monoclinic	monoclinic	monoclinic	monoclinic
space group	C2/c (No. 15)	P2 <sub>1</sub> /c (No. 14)	C2/c (No. 15)	P2 <sub>1</sub> /c (No. 14)
a [Å]	20.3963(9)	11.7373(3)	28.0667(13)	8.3232(18)
b [Å]	15.0332(6)	12.8339(3)	11.6425(5)	22.100(5)
c [Å]	23.2730(10)	13.1353(3)	17.0980(7)	14.671(4)
α [deg]	90	90	90	90
β [deg]	113.567(2)	107.6310(10)	117.051(2)	98.120(20)
γ [deg]	90	90	90	90
V [Å <sup>3</sup> ]	6540.8(5)	1885.70(8)	4975.8(4)	2671.5(12)
Z	8	8	8	4
T [K]	123	123	123	123
D <sub>calc</sub> [g cm <sup>-3</sup> ]	1.686	1.724	1.928	1.812
μ [mm <sup>-1</sup> ]	0.667	0.811	0.863	0.801
F(000)	3360	1000	2880	1448
Θ range [deg]	2.87–25.46	2.04–25.40	1.63–25.39	1.84–25.38
index ranges (h, k, l)	±24, ± 18, ± 28	±14, ± 15, ± 15	±33, -14–13, ± 20	±10, ± 26, ± 17
no. of reflns collected	63 650	61 518	43 519	59 682
no. of indep reflns/R <sub>int</sub>	6010	3463	4565	4895
no. of obsd reflns (I > 2σ(I))	5184	3102	3372	3898
no. of data/restraint/param	6010/43/484	3463/0/254	4656/0/452	4895/0/398
R1/wR2 (I > 2σ(I))	0.0453/0.1125	0.0240/0.0583	0.0416/0.0849	0.0417/0.0962
R1/wR2 (all data)	0.0546/0.1177	0.0288/0.0606	0.0697/0.0956	0.0591/0.1040
GOF (on F <sup>2</sup> )	1.032	1.026	1.024	1.025
largest diff peak/hole [e Å <sup>-3</sup> ]	1.062/-0.625	0.346/-0.231	0.691/-0.486	0.937/-0.619

Universität München. Electrospray ionization (ESI) mass spectrometry (MS) data were acquired on an LCQ-Fleet from Thermo Scientific. CV measurements were performed on a GAMRY reference 600 potentiostat, and eDAQ electrochemical reaction vessels (3 mL) were used as electrochemical cells. Platinum electrodes were used as working/counter electrodes, Ag/AgCl (3.4 M in KCl) was used as reference electrode (all from eDAQ), and ferrocene was used as internal standard. The potential is scanned with scan rates of 50 mV/s to 400 mV/s. Single crystals of 1–4 suitable for X-ray diffraction were obtained by slow diffusion of diethyl ether into an acetonitrile solution of the respective complexes (Table 2).

**Methylene Bis(trifluoromethanesulfonate) (b).** Paraformaldehyde (2.30 g, 76.6 mmol) and trifluoromethanesulfonic anhydride (21.6 g, 76.6 mmol) were mixed in a sealed Schlenk tube and heated to 80 °C for 16 h. Excess trifluoromethanesulfonic anhydride was evaporated at room temperature, giving a black residue. The crude product was filtered over a short plug of silica, using dichloromethane as a solvent. The colorless filtrate was evaporated to dryness at 20 °C to obtain the pure product as colorless oil. Yield: 5.70 g (24%). mp: 15–16 °C. <sup>1</sup>H NMR (400 MHz, CDCl<sub>3</sub>, 296 K): δ 6.06 (s, 2H, H<sub>CH<sub>2</sub></sub>) <sup>13</sup>C{<sup>1</sup>H} NMR (101 MHz, CDCl<sub>3</sub>, 296 K): δ 117.1 (q, <sup>1</sup>J<sub>CF</sub> = 320 Hz, C<sub>CF<sub>3</sub></sub>), 91.2 (s, C<sub>CH<sub>2</sub></sub>) <sup>19</sup>F NMR (376 MHz, CDCl<sub>3</sub>, 296 K): δ -74.4. Anal. Calcd for C<sub>3</sub>H<sub>2</sub>F<sub>6</sub>O<sub>6</sub>S<sub>2</sub>: C 11.54; H 0.65; F 36.52; S 20.54. Found: C 11.75; H 0.63; F 36.41; S 20.46%.

**[Calix[4]imidazolium][trifluoromethanesulfonate] (c).** A flask was charged with methylenebisimidazole (1.90 g, 12.8 mmol) and flushed with argon. The white powder was dissolved in 400 mL of dry MeCN and rigorously stirred in an ice bath. Then a solution of **b** (4.00g, 12.8 mmol) in 50 mL of dry MeCN was slowly added (1 h), and the resulting mixture was allowed to warm to room temperature. After 16 h of stirring, the clear solution was evaporated. The crude product was purified by recrystallization from acetone. After it dried under vacuum for several hours, the product was obtained as white powder (4.12 g, 70% yield). <sup>1</sup>H NMR (400 MHz, DMSO-*d*<sub>6</sub>, 296 K): δ 9.66 (s, 4H, 2-H), 8.01 (s, 8H, 4-H), 6.84 (s, 8H, CH<sub>2</sub>) <sup>13</sup>C{<sup>1</sup>H}

NMR (101 MHz, DMSO-*d*<sub>6</sub>, 296 K): δ 137.76; 123.61; 120.65 (q, <sup>1</sup>J<sub>CF</sub> = 330 Hz), 59.25. Anal. Calcd for C<sub>20</sub>H<sub>20</sub>F<sub>12</sub>N<sub>8</sub>O<sub>12</sub>S<sub>4</sub>: C 26.09; H 2.19; N 12.17; S 13.93. Found: C 25.96; H 2.16; N 11.74; S 13.75%. ESI-MS: *m/z* 770.59 [c - OTf]<sup>+</sup>, 311.03 [c - 2OTf]<sup>2+</sup>.

**[Calix[4]imidazolium][hexafluorophosphate] (d).** In a round-bottom flask, **c** (6.00 g, 6.52 mmol) was dissolved in 100 mL of deionized water and slowly added to 100 mL of a stirred aqueous solution of NH<sub>4</sub>PF<sub>6</sub> (5.31 g, 32.6 mmol). The resulting white precipitate was collected and rinsed twice with a small amount of water. The residue was dissolved in acetone and precipitated with ether. After it dried under vacuum, the product was obtained as white powder (5.3 g, 90% yield). <sup>1</sup>H NMR (400 MHz, DMSO-*d*<sub>6</sub>, 296 K): δ 9.66 (s, 4H, 2-H), 8.00 (s, 8H, 4-H), 6.84 (s, 8H, CH<sub>2</sub>). <sup>13</sup>C{<sup>1</sup>H} NMR (101 MHz, DMSO-*d*<sub>6</sub>, 296 K): δ 137.76; 123.62, 59.25 ppm. Anal. Calcd for C<sub>16</sub>H<sub>20</sub>F<sub>24</sub>N<sub>8</sub>P<sub>4</sub>: C 21.25; H 2.23; N 12.39; Found: C 20.99; H 2.15; N 12.22%. ESI-MS: *m/z* 758.70 [d - PF<sub>6</sub>]<sup>+</sup>.

**trans-Diacetonitrile[calix[4]imidazolyl]iron(II) Hexafluorophosphate (1).** A Schlenk tube was filled with [Fe{N(SiMe<sub>3</sub>)<sub>2</sub>}(THF)] (3.63 g, 8.11 mmol), and the bright green solid was dissolved in 50 mL of MeCN. The suspension was cooled to -40 °C, and via a transfer cannula 50 mL of a -40 °C cold solution of **d** (3.50 g, 3.86 mmol) was added. When the suspension warmed to room temperature, the color changed from orange over red to dark. The clear dark solution was stirred for 4 d. The resulting solution was evaporated to dryness. The remaining black residue was dissolved in 20 mL of MeCN and filtered over dried silica under argon (~15 g silica/1 g imidazolium salt used). The first orange band, eluted with MeCN, was collected, evaporated to dryness, and redissolved in 5 mL of MeCN, followed by addition of 50 mL of Et<sub>2</sub>O. Filtration gave an orange solid, which was washed twice with Et<sub>2</sub>O. After it dried under vacuum, the product was obtained as yellow powder (2.70 g, 93% yield). <sup>1</sup>H NMR (400 MHz, CD<sub>3</sub>CN, 296 K): δ 7.57 (s, 8H, CH), 6.29 (s, 8H, CH<sub>2</sub>). <sup>13</sup>C{<sup>1</sup>H} NMR (101 MHz, CD<sub>3</sub>CN, 296 K): δ 205.05 (C<sub>carbene</sub>), 122.62 (CH), 63.31(CH<sub>2</sub>). Anal. Calcd for C<sub>20</sub>H<sub>22</sub>F<sub>12</sub>FeN<sub>10</sub>P<sub>2</sub>: C 32.10; H 2.96; N 18.72. Found: C 31.91; H



3.03; N 18.56%. ESI-MS:  $m/z$  520.75 [1 – 2MeCN – PF<sub>6</sub>]<sup>+</sup>, 188.04 [1 – 2MeCN – 2PF<sub>6</sub>]<sup>2+</sup>.

**trans-Bisdimethylsulfoxid[calix[4]imidazolyl]iron(II) Hexafluorophosphate (2).** **1** (200 mg, 0.27 mmol) was dissolved in 5 mL of acetone, and DMSO (0.10 mL, 1.4 mmol) was added. The reaction mixture was stirred for 5 min at room temperature, and the solution was precipitated by addition of 10 mL of Et<sub>2</sub>O. The yellow precipitate was separated by filtration and washed twice with 5 mL of Et<sub>2</sub>O. After it dried under vacuum, the product was obtained as yellow powder (210 mg, 95% yield). <sup>1</sup>H NMR (400 MHz, CD<sub>3</sub>CN, 296 K): δ 7.64 (s, 8H, CH), 6.50 (s, 8H, CH<sub>2</sub>). <sup>13</sup>C NMR (101 MHz, CD<sub>3</sub>CN, 296 K): δ 189.31 (C<sub>carbene</sub>), 124.57 (CH), 63.96(CH<sub>2</sub>). Anal. Calcd for C<sub>20</sub>H<sub>28</sub>F<sub>12</sub>FeN<sub>8</sub>O<sub>2</sub>P<sub>2</sub>S<sub>2</sub>: C 29.21; H 3.43; N 13.63; S 7.80. Found: C 29.03; H 3.52; N 13.17%. ESI-MS:  $m/z$  520.75 [2 – 2DMSO – PF<sub>6</sub>]<sup>+</sup>, 188.04 [2 – 2DMSO – 2PF<sub>6</sub>]<sup>2+</sup>. IR (296 K): 1100 cm<sup>-1</sup> (SO).

**trans-Dicarbonyl[calix[4]imidazolyl]iron(II) Hexafluorophosphate (3).** **1** (300 mg, 0.40 mmol) was dissolved in 30 mL of dry MeCN, and the orange solution was frozen in liquid nitrogen. After evacuation, a pressure of 2.5 bar of CO was induced, and the mixture was stirred overnight at 40 °C. The bright yellow solution was concentrated to a volume of 10 mL, and addition of 50 mL of diethyl ether resulted in formation of a white precipitate. Filtration gave an off-white residue, which was washed twice with Et<sub>2</sub>O. After it dried under vacuum, the product was obtained as off-white powder (222 mg, 77% yield). <sup>1</sup>H NMR (400 MHz, CD<sub>3</sub>CN, 296 K): δ 7.55 (s, 8H, CH), 6.27 (s, 8H, CH<sub>2</sub>). <sup>13</sup>C{<sup>1</sup>H} NMR (101 MHz, CD<sub>3</sub>CN, 296 K): δ 203.82 (CO), 179.26 (C<sub>carbene</sub>), 124.49 (CH), 63.37(CH<sub>2</sub>). Anal. Calcd for C<sub>18</sub>H<sub>16</sub>F<sub>12</sub>FeN<sub>8</sub>O<sub>2</sub>P<sub>2</sub>: C 29.94; H 2.23; N 15.52. Found: C 29.96; H 2.24; N 14.71%. ESI-MS:  $m/z$  577.04 [3 – PF<sub>6</sub>]<sup>+</sup>, 549.04 [3 – CO – PF<sub>6</sub>]<sup>+</sup>. IR (296 K): 2010 cm<sup>-1</sup> (CO).

**Nitrosyl[calix[4]imidazolyl]iron(II) Hexafluorophosphate (4).** **1** (200 mg, 0.27 mmol), NaNO<sub>2</sub> (20.5 mg, 0.30 mmol), and Zn powder (9.81 mg, 0.15 mmol) were dissolved in 20 mL of dry MeCN and stirred at room temperature overnight. The resulting mixture was filtered, and the dark green filtrate was concentrated to a volume of 10 mL. Next, 40 mL of Et<sub>2</sub>O were added to precipitate a green solid, which was washed twice with Et<sub>2</sub>O and dried under vacuum. The product was obtained in 73% yield (137 mg). <sup>1</sup>H NMR (400 MHz, CD<sub>3</sub>CN, 296 K): δ 7.78 (s, 8H, CH), 6.52 (d, 4H, <sup>2</sup>J<sub>HH</sub> = 12.8 Hz, CH<sub>2</sub>), 6.46 (d, <sup>2</sup>J<sub>HH</sub> = 12.8 Hz, 4H, CH<sub>2</sub>). <sup>13</sup>C{<sup>1</sup>H} NMR (101 MHz, CD<sub>3</sub>CN, 296 K): δ 170.43 (C<sub>carbene</sub>), 124.46 (CH), 64.02(CH<sub>2</sub>). Anal. Calcd for C<sub>18</sub>H<sub>19</sub>F<sub>12</sub>FeN<sub>10</sub>O<sub>2</sub>P<sub>2</sub>: C 29.33; H 2.60; N 19.00. Found: C 29.30; H 2.63; N 19.06%. ESI-MS:  $m/z$  551.04 [4 – PF<sub>6</sub>]<sup>+</sup>. IR (296 K) 1729 cm<sup>-1</sup>.

## ■ ASSOCIATED CONTENT

### Supporting Information

Spectroscopic data of all synthesized compounds, CVs, EPR of **4**, equilibrium in deuterated solvent mixture, identification of side product, and X-ray data for **1–4** in CIF format. This material is available free of charge via the Internet at <http://pubs.acs.org>. Crystallographic data for structures **1–4** were deposited with the Cambridge Crystallographic Data Centre (CCDC 963848 (**1**) and 1036601–1036603 (**2–4**)). These coordinates can be obtained, upon request, from the Director, Cambridge Crystallographic Data Centre, 12 Union Road, Cambridge CB2 1EZ, U.K. (fax: (+44)1223–336–033; e-mail: [deposit@ccdc.cam.ac.uk](mailto:deposit@ccdc.cam.ac.uk)).

## ■ AUTHOR INFORMATION

### Corresponding Author

\*Phone: (+49) 89 289 13096. Fax: (+)49 89 289 13473. E-mail: [fritz.kuehn@ch.tum.de](mailto:fritz.kuehn@ch.tum.de).

### Notes

The authors declare no competing financial interest.

## ■ ACKNOWLEDGMENTS

M.R.A. and S.H. gratefully acknowledge support by the TUM Graduate School. This project was supported through a collaboration with the King Abdullah University of Saudi Arabia (Grant No. KSA-C0069/UKC0020).

## ■ REFERENCES

- (1) (a) Fasan, R. *ACS Catal.* **2012**, *2*, 647–666. (b) Tinberg, C. E.; Lippard, S. J. *Acc. Chem. Res.* **2011**, *44*, 280–288.
- (2) (a) Nam, W.; Lee, Y.-M.; Fukuzumi, S. *Acc. Chem. Res.* **2014**, *47*, 1146–1154. (b) Talsi, E. P.; Bryliakov, K. P. *Coord. Chem. Rev.* **2012**, *256*, 1418–1434.
- (3) (a) Riener, K.; Haslinger, S.; Raba, A.; Högerl, M. P.; Cokoja, M.; Herrmann, W. A.; Kühn, F. E. *Chem. Rev.* **2014**, *114*, 5215–5272. (b) Ingleson, M. J.; Layfield, R. A. *Chem. Commun.* **2012**, *48*, 3579–3589.
- (4) Poyatos, M.; Mata, J. A.; Peris, E. *Chem. Rev.* **2009**, *109*, 3677–3707.
- (5) (a) Kück, J. W.; Raba, A.; Markovits, I. I. E.; Cokoja, M.; Kühn, F. E. *ChemCatChem* **2014**, *6*, 1882–1886. (b) Raba, A.; Cokoja, M.; Herrmann, W. A.; Kühn, F. E. *Chem. Commun.* **2014**, *50*, 11454–11457.
- (6) Bass, H. M.; Cramer, S. A.; Price, J. L.; Jenkins, D. M. *Organometallics* **2010**, *29*, 3235–3238.
- (7) Propyl: (a) McKie, R.; Murphy, J. A.; Park, S. R.; Spicer, M. D.; Zhou, S. *Angew. Chem., Int. Ed.* **2007**, *46*, 6525–6528. (b) Findlay, N. J.; Park, S. R.; Schoenebeck, F.; Cahard, E.; Zhou, S.; Berlouis, L. E. A.; Spicer, M. D.; Tuttle, T.; Murphy, J. A. *J. Am. Chem. Soc.* **2010**, *132*, 15462–15464. (c) Lu, Z.; Cramer, S. A.; Jenkins, D. M. *Chem. Sci.* **2012**, *3*, 3081–3087. (d) Cramer, S. A.; Sanchez, R. H.; Brakhage, D. F.; Jenkins, D. M. *Chem. Commun.* **2014**, *50*, 13967–13970. (e) Cramer, A. S.; Jenkins, D. M. *J. Am. Chem. Soc.* **2011**, *133*, 19342–19345.
- (8) Meyer, S.; Klawitter, I.; Demeshko, S.; Bill, E.; Meyer, F. *Angew. Chem., Int. Ed.* **2013**, *52*, 901–905.
- (9) Chun, Y.; Singh, N. J.; Hwang, I.-C.; Lee, J. W.; Yu, S. U.; Kim, K. S. *Nat. Commun.* **2013**, *4*, 1797–1802.
- (10) Haslinger, S.; Kück, J. W.; Hahn, E. M.; Cokoja, M.; Pöthig, A.; Basset, J.-M.; Kühn, F. E. *Inorg. Chem.* **2014**, *53*, 11573–11583.
- (11) (a) Danopoulos, A. A.; Wright, J. A.; Motherwell, W. B. *Chem. Commun.* **2005**, 784–786. (b) Zlatogorsky, S.; Ingleson, M. J. *Dalton Trans.* **2012**, *41*, 2685–2693. (c) Huttner, G.; Gartzke, W. *Chem. Ber.* **1972**, *105*, 2714–2725.
- (12) (a) Gonzalez, M. A.; Fry, N. L.; Burt, R.; Davda, R.; Hobbs, A.; Mascharak, P. K. *Inorg. Chem.* **2011**, *50*, 3127–3134. (b) Stolzenberg, A. M.; Strauss, S. H.; Holm, R. H. *J. Am. Chem. Soc.* **1981**, *103*, 4763–4778. (c) Wayland, B. B.; Mehne, L. F.; Swartz, J. *J. Am. Chem. Soc.* **1978**, *100*, 2379–2383.
- (13) Sanders, B. C.; Patra, A. K.; Harrop, T. C. *J. Inorg. Biochem.* **2013**, *118*, 115–127.
- (14) (a) Berto, T. C.; Speelman, A. L.; Zheng, S.; Lehnert, N. *Coord. Chem. Rev.* **2013**, *257*, 244–259. (b) Roncaroli, F.; Videla, M.; Slep, L. D.; Olabe, J. A. *Coord. Chem. Rev.* **2007**, *251*, 1903–1930.
- (15) Ching, W.-M.; Chuang, C.-H.; Wu, C.-W.; Peng, C.-H.; Hung, J. *Am. Chem. Soc.* **2009**, *131*, 7952–7953.
- (16) (a) Scheidt, W. R.; Barabanshikov, A.; Pavlik, J. W.; Silvernail, N. J.; Sage, J. T. *Inorg. Chem.* **2010**, *49*, 6240–6252. (b) Bohle, D. S.; Hung, C.-H. *J. Am. Chem. Soc.* **1995**, *117*, 9584–9585.
- (17) (a) Raba, A.; Cokoja, M.; Ewald, S.; Riener, K.; Herdtweck, E.; Pöthig, A.; Herrmann, W. A.; Kühn, F. E. *Organometallics* **2012**, *31*, 2793–2800. (b) Danopoulos, A. A.; Braunstein, P.; Stylianides, N.; Wesolek, M. *Organometallics* **2011**, *30*, 6514–6517.
- (18) (a) Buchgraber, P.; Toupet, L.; Guerschais, V. *Organometallics* **2003**, *22*, 5144–5147. (b) Bezier, D.; Venkanna, G. T.; Sortais, J.-B.; Darcel, C. *ChemCatChem* **2011**, *3*, 1747–1750.
- (19) (a) Strauss, S. H.; Holm, R. H. *Inorg. Chem.* **1982**, *21*, 863–868. (b) Silvernail, N. J.; Noll, B. C.; Schulz, C. E.; Scheidt, W. R. *Inorg. Chem.* **2006**, *45*, 7050–7052.

- (20) (a) Hu, C.; Noll, B. C.; Scheidt, W. R. *Inorg. Chem.* **2007**, *46*, 8258–8263. (b) Hu Cheng-Bing, M.-Q.; Ma, C.-B.; Si, Y.-T.; Chen, C.-N.; Liu, Q.-T. *J. Inorg. Biochem.* **2007**, *101*, 1370–1375.
- (21) Wilkinson, G.; Gillard, R. D.; McCleverty, J. A., *Comprehensive Coordination Chemistry*, 1st ed.; Pergamon Press: Oxford, U.K., 1987.
- (22) Holleman, A. F.; Wiberg, N. *Lehrbuch der Anorganischen Chemie*, 102nd ed.; de Gruyter: Berlin, Germany, 2007.
- (23) Lee, C.-M.; Chen, C.-H.; Chen, H.-W.; Hsu, J.-L.; Lee, G.-H.; Liaw, W.-F. *Inorg. Chem.* **2005**, *44*, 6670–6679.
- (24) Alfasser, R.; Janiak, C.; Klapötke, T. M.; Meyer, H.-J. *Moderne Anorganische Chemie*; Walter de Gruyter: Berlin, Germany, 2007.
- (25) Gottlieb, H. E.; Kotlyar, V.; Nudelman, A. *J. Org. Chem.* **1997**, *62*, 7512–7515.
- (26) Enemark, J. H.; Feltham, J. H. *Coord. Chem. Rev.* **1974**, *13*, 339–406.
- (27) (a) Hsieh, C.-H.; Pulukkody, R.; Darensbourg, M. Y. *Chem. Commun.* **2013**, *49*, 9326–9328. (b) Hess, J. L.; Hsieh, C.-H.; Reibenspies, J. H.; Darensbourg, M. Y. *Inorg. Chem.* **2011**, *50*, 8541–8552. (c) Hsieh, C.-H.; Darensbourg, M. Y. *J. Am. Chem. Soc.* **2010**, *132*, 14118–14125.
- (28) Cotton, F. A.; Francis, R.; Horrocks, W. D. *J. Phys. Chem.* **1960**, *64*, 1534–1536.
- (29) Edgell, W. F.; Wilson, W. E.; Summitt, R. *Spectrochim. Acta, Part A* **1963**, *19*, 863–872.
- (30) Heinze, J. *Angew. Chem.* **1984**, *96*, 823–840.
- (31) Olmstead, M. M.; Power, P. P.; Shoner, S. C. *Inorg. Chem.* **1991**, *30*, 2547–2551.
- (32) (a) Diez-Barra, E.; de la Hoz, A.; Sanchez-Migallon, A.; Tejada, J. *Heterocycles* **1992**, *34*, 1365–1373. (b) Claramunt, R. M.; Elguero, J.; Meco, T. *J. Heterocycl. Chem.* **1983**, *20*, 1245–1249.